J Solid State Electrochem (2004) 8: 854–860
DOI 10.1007/s10008-004-0553-6

ORIGINAL PAPER

**Malgorzata Chojak · Massimiliano Mascetti
Renata Wlodarczyk · Roberto Marassi
Katarzyna Karnicka · Krzysztof Miecznikowski
Pawel J. Kulesza**

Oxidation of methanol at the network film of polyoxometallate-linked ruthenium-stabilized platinum nanoparticles

Received: 20 March 2004 / Accepted: 24 April 2004 / Published online: 12 August 2004

Abstract We explore here the ability of ruthenium hydroxo species to undergo spontaneous deposition on Pt nanoparticles and to form colloidal solutions of oxoruthenium-protected (-stabilized) nanoparticles of Pt. These particles can be spontaneously attracted to carbon substrates, and they form ultrathin self-assembled films. Fabrication of the multilayer network films on electrodes has been achieved by linking the positively charged oxoruthenium-covered Pt clusters with heteropolyanions of tungsten. By repeated alternate treatments in a solution of phosphododecatungstate ($PW_{12}O_{40}^{3-}$) and in a colloidal suspension of oxoruthenium-protected (-stabilized) Pt nanoparticles, the film thickness can be increased systematically (layer by layer) to form stable three-dimensional assemblies on carbon electrodes. It is apparent from cyclic voltammetric and chronoamperometric measurements (that were performed at 20 and 60 °C) that the resulting hybrid films show attractive properties towards the oxidation of methanol at fairly low potentials (0.25–0.4 V versus the saturated calomel electrode). With approximately the same loading of oxoruthenium-covered Pt nanoparticles and under analogous conditions, linking or derivatizing the nanoparticles with phosphotungstate leads to the system's higher electrocatalytic activity. It is possible that, in addition to ruthenium hydroxo species, $PW_{12}O_{40}^{3-}$ exhibits an activating effect on dispersed Pt particles. An alternative explanation may involve the possibility of different morphologies of the catalytic films in the presence and absence of phosphotungstate anions.

Keywords Platinum nanoparticles · Ruthenium spontaneous deposition · Phosphotungstate linking · Network electrocatalytic films · Methanol oxidation

Dedicated to Zbigniew Galus on the occation of his 70th birthday

M. Chojak · K. Karnicka · K. Miecznikowski · P. J. Kulesza (✉)
Department of Chemistry, University of Warsaw,
Pasteura 1, 02–093 Warsaw, Poland
E-mail: pkulesza@chem.uw.edu.pl

M. Mascetti · R. Wlodarczyk · R. Marassi
Dipartimento di Scienze Chimiche,
Universita di Camerino, via S. Agostino 1,
62032 Camerino (MC), Italy

R. Wlodarczyk
Division of Chemistry,
Department of Materials Engineering and Applied Physics,
Czestochowa University of Technology, Armii Krajowej 19,
42–200 Czestochowa, Poland

Introduction

The electrooxidation of methanol involves ideally six electrons per molecule to produce CO_2, and it has been extensively studied as a potential reactant for fuel cell technology during the last few years [1, 2, 3, 4, 5, 6, 7, 8, 9, 10, 11, 12, 13, 14]. During methanol oxidation, Pt shows appreciable catalytic reactivity towards C–H bond breaking, and this process is followed by several fast steps resulting in the formation of either surface CO or dissolved CO_2. Although all efficient and practical catalysts for the direct oxidation methanol fuel cell anode are based on Pt, the main problem during the electrooxidation of methanol is that the pure Pt is poisoned by strongly adsorbed CO, a by-product of methanol oxidation [15, 16, 17]. CO chemisorption significantly degrades the fuel cell performance by blocking the catalyst active sites. To prevent poisoning of Pt or to improve Pt tolerance of CO, this chemisorbed intermediate has to be removed from the surface by its oxidation to CO_2.

Pt–Ru binary metallic systems have been demonstrated to act as the best electrocatalysts for methanol oxidation [18, 19, 20, 21, 22, 23, 24, 25, 26, 27, 28]. Various mechanisms have been postulated to explain the effect of the enhancement of the methanol electrooxidation on Pt in the presence of the second metal (Ru). The phenomenon has been explained in terms of a bifunctional catalytic effect [29, 30, 31], using a ligand

model [32, 33] and so-called third-body or blocking effect [34]. It is commonly accepted that the Ru addition to Pt results in the activation of water molecules on the Ru surface to yield a metal oxo species of the type Ru–OH. Thus the CO intermediate can react with the Ru–OH species to yield CO_2:

$$Pt - CO + Ru - OHPt + Ru + CO_2 + H^+ + e^-. \quad (1)$$

An important issue is that pure Ru forms surface hydroxides at potentials starting from 0.3 V versus the standard hydrogen electrode, i.e., lower in comparison with Pt (0.6 V versus the standard hydrogen electrode). Consequently, the removal of CO should be much faster on the Pt–Ru surface than on pure Pt. Introduction of foreign metal atoms may also increase the Pt activity owing to changes in electronic interactions and adsorption properties. According to the ligand model the main role of Ru is to modify the electronic structure of the Pt surface by interacting with the conduction band of Pt. Thus, the Pt–CO bond is expected to be weakened and so less energy would be required to oxidize the adsorbed CO. It is usually accepted that the ratios of Ru to Pt in a binary catalyst ranging from 10 to 50% provide enough Pt and Ru sites for the effective oxidation of methanol [9].

Binary Pt–Ru catalysts proposed for the oxidation of methanol have the following forms: Pt–Ru alloys [23, 24], Ru electrodeposits on Pt [35, 36], Pt–Ru codeposits [37, 38] and Ru adsorbed on Pt [40, 41, 42]. An interesting alternative originates from the possibility of the preparation of binary Pt–Ru electrocatalysts as a result of spontaneous adsorption of Ru on a surface Pt single crystal or Pt black [39, 40, 41].

There are numerous examples of electrocatalytic modified electrodes in which reactive centers are three-dimensionally distributed within thin films attached to an electrode substrate [42, 43, 44, 45, 46, 47, 48, 49, 50, 51, 52, 53, 54]. Immobilization of metal nanoparticles embedded in a porous matrix results in an increase of the catalytic metal specific area [55, 56, 57, 58, 59, 60]. An important practical issue is the stabilization of nanoparticles that prevents their agglomeration, leading to the gradual loss of activity. In the case of gold nanoparticles, recent attention has focused on the formation of alkanethiolate monolayer-protected clusters. Self-assembled alkanothiolates on gold tend to separate Au nanoparticles and reduce their agglomeration [61, 62]. Very recently, we have demonstrated that Pt nanoparticles can be stabilized with polyoxometallates by exploring their ability to form stable anionic monolayers on solid surfaces [63, 64]. The resulting polyoxometallate-protected (-stabilized) Pt nanoparticles can be subsequently linked with ultrathin conducting polymer layers to form network films.

In the present work, we extend the layer-by-layer method to linking Ru-stabilized (-covered) Pt nanoparticles with polyoxometalates to form electrocatalytic network films. Polyoxometalates are metal clusters coordinated by bridging oxygen atoms forming well-defined structures that undergo a reversible multielectron reduction process [65].

We explore here the fact that Ru oxo species adsorbed on Pt nanoparticles are positively charged and they are expected to interact with anionic phosphododecatungstate (PW_{12}) [66]. The results are consistent with the view that PW_{12} does not only stabilize the Ru-decorated Pt nanoparticles but also enhances the methanol oxidation currents under chronoamperometric conditions.

Experimental

All chemicals were commercial materials of analytical grade purity and were used without further purification. Pt black clusters (surface area, 20 $m^2\ g^{-1}$) were obtained from Johnson & Matthew. Solutions were prepared using doubly-distilled and subsequently deionized (Millipore Milli-Q) water. Argon was used to deaerate the solutions and to keep an air-free atmosphere over the solution during the measurements. Unless otherwise stated, all experiments were performed at room temperature (about 20 °C).

Electrochemical measurements were done with a CH Instruments (Austin, USA) model 650 workstation. A standard three-electrode cell was used for all experiments. Toray Teflon-treated carbon paper (geometric surface area, 0.7 cm^2) from Electrochem (Woburn, USA) served as the working electrode and Pt wire as the counter-electrode. All potentials were expressed versus the saturated (KCl) calomel electrode.

To produce a colloidal (sol-type) Pt–Ru solution of Ru-covered Pt nanoparticles, a suspension of a known amount (0.33 g) of Pt black was formed in 10 cm^3 5 mmol dm^{-3} $RuCl_3$ solution (pH≈4). The suspension was left for about 48 h to permit formation of Ru oxo (hydroxo) species (from $RuCl_3$) and their spontaneous deposition [39, 40, 41] on the surfaces of Pt nanoparticles. Subsequently, it was sonicated for 1 h and, then, centrifuged. The solution was decanted 2–3 times, and the final colloidal solution (sol) of oxoruthenium-covered (-stabilized) Pt nanoparticles was made in water.

The network film was assembled through the alternate immersions scheme (layer by layer) in a manner analogous to that described previously [63, 64]. The Teflon-treated carbon paper (working electrode) was serially exposed to the Pt–Ru solution: for about 24 h to obtain the first layer of oxoruthenium-coated Pt nanoparticles and, subsequently, for 30 min in the following (typically three) steps. Between the steps of the layer-by-layer procedure, the electrode was exposed to 3 mmol dm^{-3} PW_{12} solution for 10 min. As a rule, the electrode was rinsed with water after the formation of each layer. Following preparation, the modified electrode was characterized by recording a cyclic voltammogram in 0.5 mol dm^{-3} H_2SO_4. While the loading of Pt in the initial layer of oxoruthenium-coated Pt nanoparticles was on the level of 0.04 mg cm^{-2}, approximately

0.02 mg cm^{-2} Pt was added upon fabrication of each additional layer. Apparently, the initial attachment or chemisorption of Ru-coated Pt nanoparticles to bare carbon was more pronounced than their further electrostatic attraction by polytungstate linkers.

The morphology of the electrocatalytic films was monitored using a Philips CM 10 scanning transmission electron microscope (TEM) operating at 100 kV. The samples were also subjected to energy-dispersive analysis by an X-ray unit coupled with a JEOL model JSM-5400 scanning electron microscope. The amount of Pt in the catalytic films was determined (following digestion of the films in aqua regia) using the spectrophotometric approach reported earlier [67]. The method permits determination of Pt in the presence of Ru. Film loadings, expressed as surface coverages of Ru species (in moles per centimeter squared), were estimated upon determination of the charges under the system's reduction voltammetric peaks recorded at a slow scan rate, 5 mV s^{-1}.

Results and discussion

Formation of network films of Ru-stabilized Pt nanoparticles

The procedure of stabilizing Pt nanoparticles and protecting them from agglomeration by modification with a Ru layer involved exposure of Pt clusters to $RuCl_3$ solution as described in the Experimental section. The actual modification step should be interpreted in terms of interfacial interaction and adsorption of the Ru oxo or hydroxo cations, including $RuO[(H_2O)_4]^{2+}$ that exist in the aged $RuCl_3$ solution, on the Pt particles [9, 10, 11, 12, 13, 14, 15, 16, 17, 18, 19, 20, 21, 22, 23, 24, 25, 26, 27, 28, 29, 30, 31, 32, 33, 34, 35, 36, 37, 38, 39, 40, 41]. When an aliquot of a colloidal solution of oxoruthenium-covered Pt nanoparticles was placed on a grid, subjected to drying and, subsequently, to the TEM examination (Fig. 1a), it became apparent that the system forms aggregates composed of smaller units, presumably the Ru-covered Pt nanoparticles of approximate size 10–15 nm. Apparently, the existence of electrostatic repulsive interactions between the positively charged Ru oxo species deposited on the Pt surfaces led to the formation of well-separated nanostructures (clusters) in solution.

Since the positively charged Ru oxo species (deposited on Pt nanoparticles) can interact with heteropolytungstate anions [66], the particles can be further derivatized and stabilized with PW_{12}. The procedure involves exposure of the oxoruthenium-covered Pt particles to PW_{12} solution, consecutive centrifuging and washing off with water to form a colloidal suspension of PW_{12}-derivatized Ru-covered nanosized Pt. The presence of W, Ru and Pt was confirmed from the energy-dispersive X-ray elemental analysis. The TEM image of the resulting particles deposited on a grid is illustrated in Fig. 1b. As in the case of Fig. 1a, the specimen forms

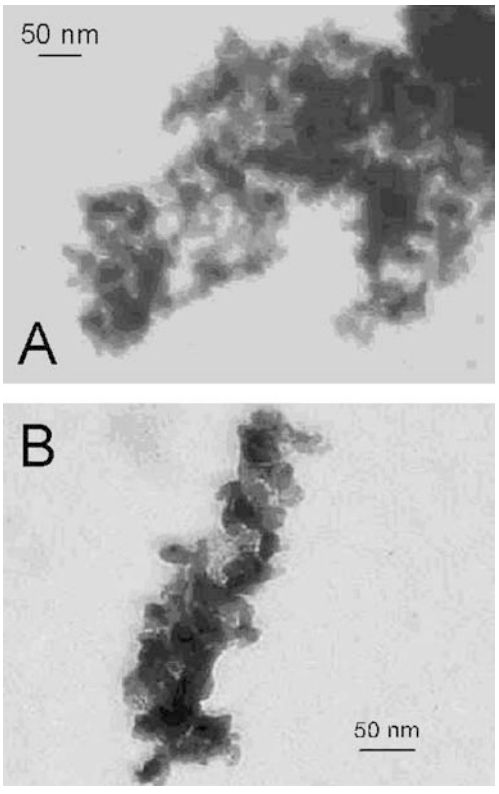

Fig. 1 Transmission electron microscope images of **a** oxoruthenium-coated and **b** phosphododecatungstate (PW_{12})-derivatized and oxoruthenium-coated clusters of Pt nanoparticles

aggregates composed of smaller units (particles) typically of about 15 nm. Despite the fact that the macrostructures of the aggregates are different (they were randomly chosen), the size of the clusters in Fig. 1b is comparable to that in Fig. 1a because derivatization with tetragonal phosphotungstate of about 1.2 nm is not expected to change significantly the particle diameter. From the data of Fig. 1a and b, we find that there is some degree of heterogeneity in the dispersion of PW_{12}-derivatized oxoruthenium coated Pt particles.

Typical cyclic voltammetric responses (recorded in argon-saturated 0.5 mol dm^{-3} H_2SO_4) of carbon paper electrodes modified with ultrathin films of the simple Pt catalyst (curve a) and Ru-covered Pt nanoparticles (curve b) are shown in Fig. 2a. While in the case of curve a, the electrode preparation procedure involved simple placing of an aliquot of the pure Pt nanoparticle suspension as described elsewhere [57], the fabrication of Ru-covered Pt nanoparticles on carbon paper (curve b) was achieved by simple dipping of the electrode substrate in the Pt–Ru colloidal solution. We believe that the attachment of Pt nanoparticles to carbon paper was facilitated by the presence of Ru oxo species capable of chemisorbing on both Pt and carbon substrates. It is noteworthy that the voltammetric pattern of the oxoruthenium covered Pt nanoparticles (curve b) exhibits both peaks characteristic of Ru oxo species (at potentials larger than 0.3 V) and those typical of

hydrogen adsorption (originating from the presence of catalytic Pt) at potentials more negative than 0.1 V. When compared with the response of a Ru oxide film on carbon paper (Fig. 2b, curve a), that was generated by aging in $RuCl_3$ solution, the film of Ru-covered Pt nanoparticles (Fig. 2a, curve b) exhibits Ru oxo transitions at more positive potentials, namely closer to those characteristic of the Pt/PtO system. It is reasonable to expect that, in the latter case, the generation of Ru oxo species at oxidation states higher than II [68] is mediated by formation of Pt oxides. Another possibility takes into account the existence of mutual ineraction and formation of mixed oxides. Both Ru and Pt oxides undergo electrochemical reactions by reversibly accepting protons from or donating protons to aqueous supporting electrolyte.

Following the formation of the initial film of Ru-coated Pt nanoparticles on the carbon paper substrate, the multilayer film was generated layer by layer by alternately exposing the electrode surface to 3 mmol dm^{-3} PW_{12} and to the colloidal Pt–Ru solution. The successful formation of the multilayer (network) film consisting of Pt–Ru and PW_{12} is demonstrated by the increase of the voltammetric peak currents (Fig. 3) following alternate treatments in colloidal suspensions of Ru-decorated Pt nanoparticles and the PW_{12} solution. Higher currents at potentials lower than 0.1 V are attributed to the growth of not only hydrogen adsorption/desorption peaks (owing to increasing the number of Pt nanoparticle layers) but also to the electroactivity of the alternately and systematically attracted PW_{12} redox centers (layers). It is apparent from Fig. 2b, curve b that, in the potential range, from 0.1 to −0.2 V, the adsorbed PW_{12} (on carbon paper) is characterized by a well-defined redox reaction [69] that can be described as follows:

$$PW_{12}^{VI}O_{40}^{3-} + e^- \rightarrow PW^{V}W_{11}^{VI}O_{40}^{4-}. \quad (2)$$

Thus, the voltammetric peaks at about −0.1 V (Fig. 3) mirror the overlapping contributions from both the first one-electron reduction of PW_{12} and the hydrogen surface processes on Pt. The increase of currents at potentials higher than 0.3 V (Fig. 3) reflects the electroactivity of the increasing amounts of the alternately deposited Ru-covered Pt nanoparticles.

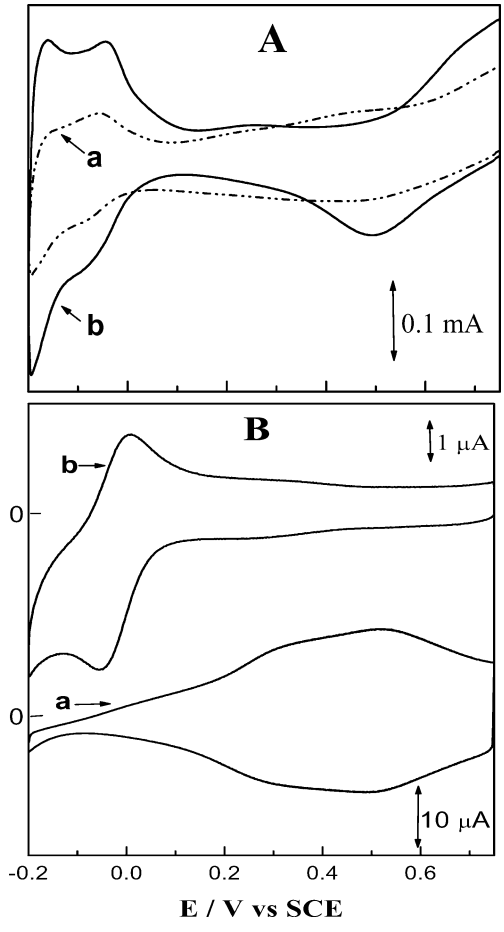

Fig. 2 Cyclic voltammetric responses of **a** bare Pt nanoparticles (*a*) and oxoruthenium coated Pt (*b*) nanoparticles attached to a carbon paper electrode and **b** PW_{12} chemisorbed on glassy carbon (*a*) and Ru oxo species deposited from aged in $RuCl_3$ solution on glassy carbon (*b*) (geometric surface area, 0.071 cm^2). Scan rate, 50 mV s^{-1}. Electrolyte, 0.5 mol dm^{-3} H_2SO_4

Methanol oxidation at the network film

We addressed the system's electrocatalytic properties by examination of the reactivity of a multilayer film towards oxidation of methanol. The voltammetric results of Fig. 4 show that PW_{12}-linked and Ru-oxo species covered Pt nanoparticles (characterized by curve a, which was recorded in supporting electrolyte only) catalyze the oxidation of methanol (curve b). The overall process can be summarized [13]:

$$CH_3OH + H_2O \rightarrow CO_2 + 6H^+ + 6e^-. \quad (3)$$

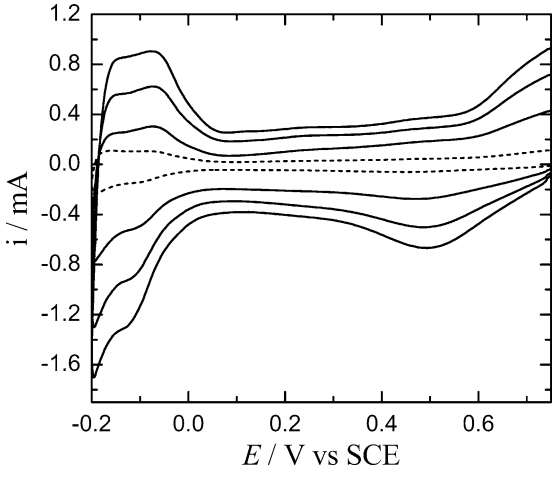

Fig. 3 Voltammetric monitoring of the growth (layer by layer) of the network film of PW_{12}-linked oxoruthenium-coated Pt nanoparticles (on carbon paper). Dotted line shows cyclic voltammogram of the initial layer of oxoruthenium-coated Pt. Scan rate, 50 mV s^{-1}. Electrolyte, 0.5 mol dm^{-3} H_2SO_4

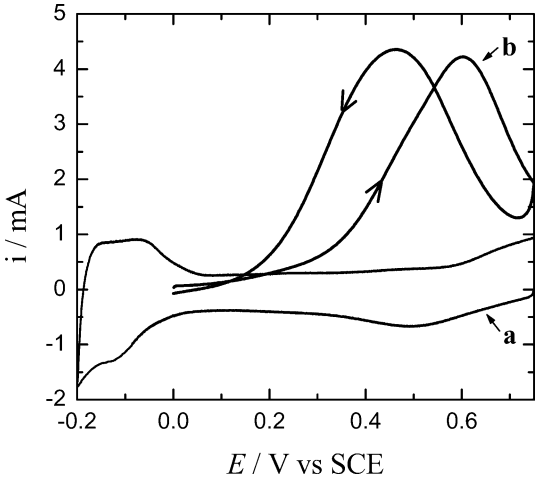

Fig. 4 Cyclic voltammetric responses of the network film (as for Fig. 3) of PW_{12}-linked oxoruthenium-coated Pt nanoparticles in the absence (*a*) and in the presence (*b*) of 0.1 mol dm^{-3} methanol. Scan rate, 50 mV s^{-1}. Electrolyte, 0.5 mol dm^{-3} H_2SO_4. Curve b was recorded following preconditioning for 60 s at 0 V

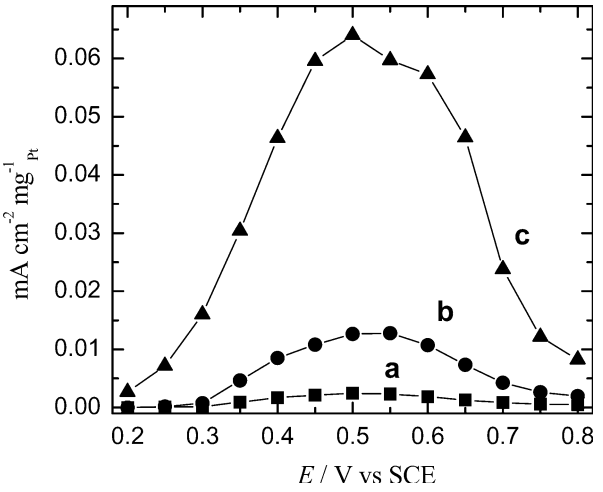

Fig. 5 Staircase voltammetric current densities (normalized per 1 mg of Pt catalyst) for the methanol (0.1 mol dm^{-3}) oxidation recorded every 50 mV (between 0.2 and 0.8 V) following application of 50-s potential steps at the initial layer of oxoruthenium-coated Pt nanoparticles (*a*), the same layer but the particles were further derivatized with PW_{12} (*b*) and a multilayer film (as for Fig. 3) of PW_{12}-linked oxoruthenium-coated Pt nanoparticles on carbon paper (*c*). Temperature, 20 °C. Electrolyte, 0.5 mol dm^{-3} H_2SO_4

As expected, during the reverse (negative) potential scan, additional methanol oxidation voltammetric currents are observed. Such behavior is analogous to what was previously observed at binary Pt–Ru catalysts [13, 57]. An important issue of the data of Fig. 4 is that the methanol oxidation currents tend to appear at less positive potentials than on bare Pt [54, 57].

To get better insight into the system's reactivity towards oxidation of methanol, we considered the dependencies of staircase (step period of 50 s) voltammetric responses (related to the oxidation of methanol) on the loadings of (Ru-coated) Pt in the network films (Fig. 5). The main features obvious from these relationships are as follows. As expected, a significant increase of electrocatalytic currents was observed upon formation of the additional layer of oxoruthenium-covered Pt nanoparticles (compare curves b and c), namely upon increase of the total loading of Pt from about 0.04 to 0.09 mg cm^{-2}. The Ru component is in excess, and its molar ratio to Pt was found, in general, to be approximately 2:1. We also found that simple derivatization of the ultrathin film of Ru-covered Pt nanoparticles by exposing them to PW_{12} results in some increase of the methanol electrocatalytic currents (compare curves a and b in Fig. 5). This finding can be rationalized in terms of the relative availability, potential mutual interactions, and the existence of sufficient numbers of neighboring Pt and Ru centers for efficient oxidation of methanol. Although, we have no evidence for any direct reactivity of PW_{12}, an alternative explanation of the enhancement effect may originate from the fact that the PW_{12} heteropolycompound is analogous to the parent tungsten oxide. It should be remembered that the electrodeposited Pt/WO_3 coatings have been demonstrated to act as effective anode materials for the direct oxidation methanol fuel cell [46, 54, 70]. One can also take into account morphological differences (particularly with respect to dispersed Pt) between Ru-covered Pt and Ru-covered Pt derivatized with PW_{12}. Although TEM results do not support this view (dispersion of Pt was approximately the same in both cases), such a possibility cannot be excluded.

When the temperature was increased from 20 (Fig. 5) to 60 °C (Fig. 6), the analogous current–potential responses were recorded except that the electrocatalytic current densities approximately doubled. This result is not surprising because, at higher temperatures, the degree of poisoning of Pt by the methanol oxidation intermediate is lower and Ru oxo species are expected to utilize more effectively –OH groups or radicals capable

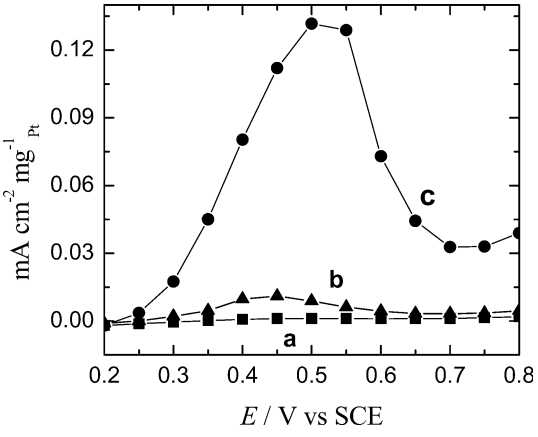

Fig. 6 Staircase voltammetric current densities recorded as for Fig. 5 except that the temperature was increased to 60 °C

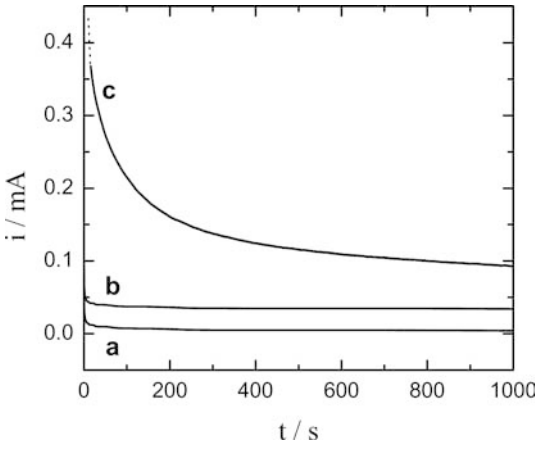

Fig. 7 Chronoamperometric responses for the methanol oxidation (0.3 V; 20 ″C) at the initial layer of oxoruthenium-coated Pt nanoparticles (*a*), the same layer but the particles were further derivatized with PW_{12} (*b*) and a multilayer film (as for Fig. 3) of PW_{12}-linked oxoruthenium-coated Pt nanoparticles on carbon paper (*c*). Electrolyte and methanol concentrations as for Fig. 5

of facilitating oxidation of passivating intermediates (CO_{ads}) on Pt.

To evaluate further the reactivity of our electrocatalytic system for the methanol oxidation, current–time measurements were performed (Fig. 7). The results show that the steady-state methanol oxidation currents can be developed under the conditions of chronoamperometric experiments. By analogy to the data of Figs. 5 and 6, the growth of the network (multilayer) film by alternate immersions in Pt–Ru and PW_{12} solutions results in an increase of the methanol electrooxidation currents. Current–time measurements recorded at different constant potentials (0.25, 0.30 or 0.40 V) are illustrated in Fig. 8. Although, as expected, the largest currents are observed at the most positive potential applied (curve c), it is noteworthy that the steady-state currents were still developed at more negative potentials (curves a and b).

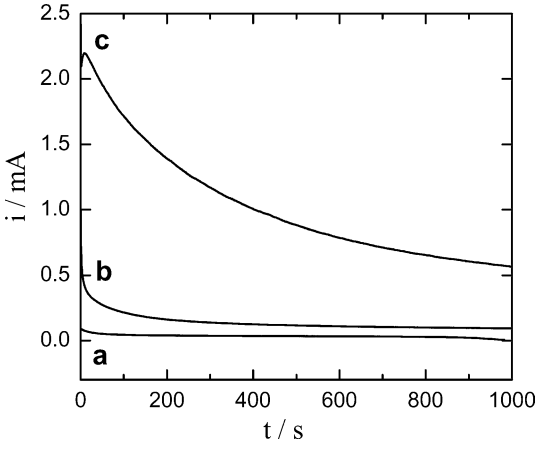

Fig. 8 Chronoamperometric curves recorded for the methanol oxidation at a multilayer film (as for Fig. 3) of PW_{12}-linked oxoruthenium-coated Pt nanoparticles on carbon paper upon application of (a) 0.25 V (*a*), 0.30 V (*b*) and 0.40 V (*c*). Other conditions as for Fig. 7

Conclusions

We demonstrated the usefulness of the layer-by-layer method for the fabrication of hybrid films composed of heteropolyanion (PW_{12}) linked oxoruthenium-coated Pt nanoparticles. The approach seems to provide a novel concept of assembling bimetallic Pt–Ru nanoparticles (using polyoxometallate linkers) to form the network electrocatalytic structures.

We also found that the derivatization of oxoruthenium coated Pt nanoparticles with phosphotungstate enhances (certainly not decreases) the activity of dispersed electrocatalyst towards electrooxidation of methanol in acid solution. Although no direct comparison of our system with the activity of commercial Vulcan-supported binary Pt–Ru catalyst was made here (owing to the distinct morphologies and metal loadings in both catalysts), our preliminary results show that the network film of polyoxometallate-linked Ru-stabilized Pt nanoparticles seems to be promising for the formation of the anode catalyst. This catalytic enhancement may be due to the synergistic effect between Pt–Ru and PW_{12}. Having in mind the activity of tungsten oxides [70], tungstate units may provide additional –OH groups or radicals capable of facilitating oxidation of passivating intermediates (CO_{ads}) on Pt. Alternatively, introduction of PW_{12} may induce morphological differences and lead to better Pt catalyst utilization. Further research is necessary to optimize the distribution and the size of PW_{12}-derivatized and linked oxoruthenium-coated Pt nanoparticles.

Acknowledgements This work was supported by the State Committee for Scientific Research (KBN), Poland, under grant 7 T09A 05426 and by the Ministerio dell'Istruzone dell'Universita e della Ricerca, Italy, under grant FISR 2000. Support from the exchange program between the universities in Camerino and Warsaw is also appreciated. K.M. was supported in part by the University of Warsaw under the BW project. M.C. acknowledges a fellowship from the Foundation for Polish Science (FNP).

References

1. Bagotzky VS, Vassiliev YB, Khazova OK (1977) J Electroanal Chem 81:229
2. Clavilier J, Lamy C, Leger JM (1981) J Electroanal Chem 1250:249
3. Parson R, Van der Noot T (1988) J Electroanal Chem 125:9
4. Adzic R, (1990) In: Bockris JO'M, Conway BE, White RE (eds) Modern aspects of electrochemistry, vol 21. Plenum, New York
5. Stonehart PJ (1992) J Appl Electrochem 22:995
6. Kizhakevariam N, Stuve EM (1993) Surf Sci 286:246
7. Herrero E, Franaszczuk K, Wieckowski A (1994) J Phys Chem 98:5074
8. Markovic N, Ross PN (1992) J Electroanal Chem 330:499
9. Iwasita T, Hoster H, John-Anacer A, Lin WF, Vielstich W (2000) Langmuir 16:522
10. Petrii OA, Podlovchenko BI, Frumkin AN, Lal H (1968) J Electroanal Chem 10:253
11. Kurimatsu K (1990) Ber Bunsenges Phys Chem 94:1025
12. Cameron RS, Hards GA, Harrison B, Porter RJ (1987) Platinum Met Rev 31:17

13. Hamnett A (1999) In: Wieckowski A (ed) Interfacial electrochemistry: theory, experiment and applications. Dekker, New York
14. Wasmus S, Kuwer A (1999) J Electroanal Chem 461:14
15. Leger JM, Lamy C (1990) Ber Bunsenges Phys Chem 94:1021
16. Morimoto Y, Yeager EB (1998) J Electroanal Chem 444:95
17. Mc Breen J, Mukerjee S (1995) J Electrochem Soc 142:3399
18. Beden B, Kardigan F, Lamy C, Leger JM (1981) J Electroanal Chem 127:75
19. Ross PN, Gasteiger HA Jr (1995) In: Savadogo O (ed) New materials for fuel cell systems 1. Editions de L'Ecole Polytechnique de Montreal, Montreal
20. Gasteiger HA, Markovic N, Ross PN, Cairns EJ Jr (1993) J Phys Chem 97:12020
21. Chu D, Gilman S (1996) J Electrochem Soc 143:1685
22. Chrzanowski W, Kim H, Tremiliosi-Filho G, Grzybowska B, Kulesza PJ (1998) J New Mater Electrochem Syst 1:31
23. Markovic NM, Gasteiger HA, Ross PN Jr, Jiang X, Villegas I, Weaver MJ (1995) Electrochim Acta 40:91
24. Gasteiger HA, Markovic N, Ross PN, Cairns EJ Jr (1994) J Electrochem Soc 141:1795
25. Lima A, Countanceacy C, Leger J-M, Lamy C (2001) J Appl Electrochem 31:379
26. Lu C, Rice C, Masel RJ, Babu PK, Waszczuk P, Kim HS, Oldfield E, Wieckowski A (2002) J Phys Chem B 106:9581
27. Iwasita T, Hoster H, John-Anacker A, Lin WF, Vielstich W (2000) Langmuir 16:522
28. Babu PK, Kim HS, Oldfield E, Wieckowski A (2003) J Phys Chem B 107:7595
29. Watanabe M, Motoo S (1975) J Electroanal Chem 60:259
30. Liu R, Ley KL, Pu C, Fan Q, Leyarovska N, Segre C, Smotkin ES (1996) In: Wieckowski A, Itaya K (eds) Electrode processes VI, Electrochemical Society proceedings, vol 96–98. Electrochemical Society, Pennington, p 34
31. Gasteiger HA, Markovic N, Ross PN, Cairns EJ (1993) J Phys Chem 97:12020
32. Janssen MMP, Moolhuysen J (1977) J Catal 46:289
33. Janssen MM, Moolhuysen J (1976) Electrochim Acta 21:869
34. Angestein-Kozlowska H, MacDougall B, Conway BE (1973) J Electrochem Soc 120:756
35. Friedrich KA, Geyzers KP, Linke W, Stimming U, Stumper J (1996) J Electroanal Chem 402:123
36. Chrzanowski W, Wieckowski A (1998) Langmuir 14:1967
37. Krause M, Vielstich W (1994) J Electroanal Chem 379:307
38. Hogarth MP, Munk J, Shukla AK, Hamnett A (1994) J Appl Electrochem 24:85
39. Chrzanowski W, Kim H, Wieckowski A (1998) Catal Lett 50:69
40. Crown A, Johnston C, Wieckowski A (2002) Surf Sci 506:L268
41. Fachini ER, Diaz-Ayala R, Casado-Rivera E, File S, Cabrera CR (2003) Langmuir 19:8986
42. Kulesza PJ, Matczak M, Wolkiewicz A, Grzybowska B, Galkowski M, Malik MA, Wieckowski A (1999) Electrochim Acta 44:2131
43. Kostecki R, Ulmann M, Augustynski J, Strike DJ, Kondelka-Hep M (1993) J Phys Chem 97:8113
44. Wilson MS, Gottesfeld S (1992) J Electrochem Soc 139:L28
45. Pickup PG, Kuo N, Murray RW (1983) J Electrochem Soc 130:2205
46. Kulesza PJ, Faulkner LR (1989) J Electroanal Chem 259:81
47. Bose CSC, Rajeshwar K (1992) J Electroanal Chem 333:235
48. Bortak ED, Kazce B, Shimaze K, Kuwana T (1988) Anal Chem 60:2379
49. Chandler GK, Pletcher D (1986) J Appl Electrochem 16:62
50. Vork FTA, Barendrecht E (1990) Electrochim Acta 35:135
51. Bedioni F, Voision M, Derynck J, Bied Charreton C (1991) J Electroanal Chem 297:257
52. Laborde H, Legger JM, Lamy C (1994) J Appl Electrochem 24:219
53. Chen KY, Tseung ACC (1996) J Electrochem Soc 143:2703
54. Kulesza PJ, Grzybowska B, Malik MA, Chojak M, Miecznikowski K (2001) J Electroanal Chem 512:4371
55. Park S, Yang P, Corredor P, Weaver MJ (2002) J Am Chem Soc 124:2428
56. Charette L, Friedrich KA, Stimming U (2000) Chem Phys Chem 1:162
57. Waszczuk P, Solla-Gullon J, Kim H-S, Tong YY, Montiel V, Aldaz A, Wieckowski A (2001) J Catal 203:1
58. McBreen J, Mukerjee S (1999) In: Wieckowski A (ed) Interfecial electrochemistry. Dekker, New York, p 895
59. Reetz MT, Lopez M, Grunert W, Vogel W, Mahlendorf F (2003) J Phys Chem B 107:7414
60. Gao L, Huang H, Korzeniewski C (2004) Electrochim Acta 49:1281
61. Zamborini FP, Leopold MC, Hicks JF, Kulesza PJ, Malik MA, Murray RW (2002) J Am Chem Soc 124:8958
62. Chen SW, Ingram RS, Hostetler MJ, Pietron JJ, Murray RW, Schaaff TG, Khoury JT, Alvarez MM, Whetten RL (1998) Science 280:2098
63. Kulesza PJ, Chojak M, Miecznikowski K, Lewera A, Malik MA, Kuhn A (2002) Electrochem Commun 4:510
64. Kulesza PJ, Chojak M, Karnicka K, Miecznikowski K, Palys B, Lewera A, Wieckowski A Chem Mater (submitted)
65. Pope MT (1983) Heteropoly and isopoly oxometalates. Springer, Berlin Heidelberg New York
66. Kulesza PJ, Roslonek G, Faulkner LR (1990) J Electroanal Chem 280:233
67. Balcerzak M, Swiecicka E, Balukiewicz E (1999) Talanta 48:39
68. Zheng JP, Cygan PJ, Jow TR (1995) J Electrochem Soc 142:2699
69. Kulesza PJ, Karwowska B, Malik M (1998) Colloids Surf A 134:173
70. Shen PK, Tseung ACC (1994) J Electrochem Soc 141:3082